Transient wave propagation analysis of a pantograph-catenary system

Kyohei Nagao and Arata Masuda

Department of Mechanical and System Engineering, Kyoto Institute of Technology, Matsugasaki, Sakyo-ku, Kyoto, Japan

E-mail: masuda@kit.ac.jp

Abstract. This paper proposes a systematic method to analyze the dynamic response of an overhead catenary with pantographs moving at constant speed. The overhead catenary is modeled as a one-dimensional infinite-length string, which is periodically supported by hangers. On the other hand, the pantograph is a sub-structure moving at a constant speed, which is modeled as a lumped mass system contacting the catenary. In this study, the whole system is divided into elements in the manner of the transfer matrix method. Then, the relationship among traveling waves in every element is systematically obtained in the Laplace domain following the method of reverberation-ray matrix. Since the governing equation of the system changes periodically with time, the analysis of the temporal evolution of the system can be realized by repeating a single period analysis starting from the instant when the pantograph comes into a unit cell by means of the reverberation-ray matrix analysis followed by the inverse Laplace transform. When the pantograph reaches the opposite hanger, the whole elements are shifted backward, and the catenary response of the forehead element is used as the initial condition of the next period.

1. Introduction

An overhead catenary system is a complex, elongated, almost periodic and infinite structure which supplies current to a train vehicle through pantographs. The pantograph which is a structural system moving along the catenary experiences complex dynamic interaction with the catenary system especially in high speed range. Since the stability of the contact force between the catenary and the pantograph is a critical factor for reliability of the current collection and reduction of the maintenance cost, fully understanding of the coupled behavior of the catenary-pantograph system is essential for high-speed railway.

The catenary-pantograph system has the following characteristics which may lead to difficulties in developing an analysis method:

- it can be modeled as a structure with infinite length;
- the pantograph itself is a dynamical system interacting with the catenary as a moving sub-structure;
- not only its steady-state response but also the transient response is of interest.

A number of studies were conducted in the past on analyses of similar types of coupled systems. Gilbert and Davies [1] studied the steady-state responses of the catenary system modeled as a string supported by continuous elastic medium whose stiffness periodically varied along the line. The pantograph was modeled both as zero impedance, i.e., a simple force, and as a lumped mass system. Scott and Rothman [2] presented a numerical study using a lumped parameter model of catenary and pantographs. Smith


Content from this work may be used under the terms of the Creative Commons Attribution 3.0 licence. Any further distribution of this work must maintain attribution to the author(s) and the title of the work, journal citation and DOI.
Published under licence by IOP Publishing Ltd

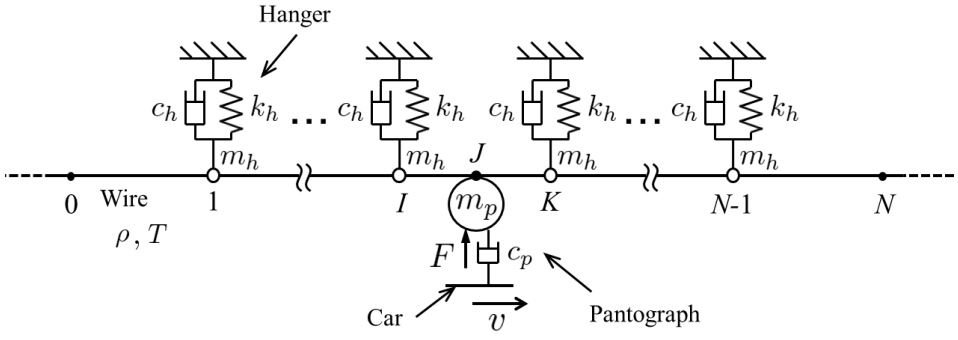


Figure 1. Analysis model of pantograph-catenary system.

and Wormley [3] presented an analysis of periodically supported continuous beam with moving load. Metrikine el al. [4] analytically derived steady-state solutions of periodically supported structure under a moving load using periodicity condition. The same approach was applied to a two-level catenary under a moving load [5, 6]. These analyses did not take the dynamical behavior of the pantograph into account. On the other hand, Bitzenbauer and Dinkel [7] dealt with an infinite beam supported by homogeneous elastic medium coupled with a moving multi-degree-of-freedom structure based on double Fourier transform. This work did not take account of the spatial periodicity. Shimogo et al. [8] formulated a steady-state response of a periodically suspended catenary with a moving pantograph assuming periodicity condition. To the best of authors' knowledge, however, there is no existing methods presented in the literature which can deal with all of the three characteristics.

In this paper, a Laplace transform-based semi-analytical approach to this challenge is presented. The catenary is modeled as an infinite-length string periodically supported by hangers which are modeled by lumped masses, springs and dampers. The pantograph is modeled as a lumped mass system moving at a constant speed contacting the catenary. The whole system is divided into elements on the basis of transfer matrix method [9, 10]. Then, the relationship among traveling waves in every element is systematically obtained in the Laplace domain in terms of a method of reverberation-ray matrix [11, 12, 13]. The method of reverberation-ray matrix is a numerical method originally developed to analyze transient elastic waves in a planar truss [11] in which a lot of members are inter-connected to form a network-like structure. It is based on tracking of wave propagation in the structure using the exact solutions of traveling waves, therefore it is a numerical shceme free from discretization errors and intrinsically stabile.

Since the governing equation of the system changes periodically with time, the analysis of the temporal evolution of the system can be realized by repeating a single period analysis starting from the instant when the pantograph comes into a unit cell by means of the reverberation-ray matrix analysis followed by the inverse Laplace transform. Since all the formulations are constructed based on wave component representation, wave propagation phenomena such as reflection, transmission at discontinuities and Doppler effect at the pantograph can be effectively taken into account.

2. Modeling

2.1. Governing equations

Typical catenary system consists of a contact wire from which the pantograph receives electricity, a carrying wire which suspends the contact wire, and periodically placed hangers which vertically connect two wires. In this study, the carrying wire is omitted from the model for the simplicity, and the flexibility of the carrying wire is represented by the flexibility of the hangers. Furthermore, only single pantograph is considered. It should be noted here that it would be relatively easy to implement a full pantograph-catenary model involving the carrying wire and multiple pantographs because the methodology developed in this study is systematic and independent of any specific model structures.

The analysis model in this study is illustrated in figure 1. It consists of a contact wire supported by hangers and a moving pantograph. The contact wire is modeled as an infinite-length string which is governed by a wave equation given by

$$\rho\frac{\partial^2 y(x,t)}{\partial t^2} - T\frac{\partial y(x,t)}{\partial x^2} = 0 \tag{1}$$

where $y(x,t)$ is the vertical displacement of the wire at horizontal location x and time t; ρ and T are the linear density and tension of the contact wire, respectively. The internal force of the wire is defined as

$$V(x,t) = -T\frac{\partial y(x,t)}{\partial x} \tag{2}$$

The hanger are modeled by uniform single-degree-of-freedom lumped mass systems whose equation of motion is given by

$$m_h\frac{d^2 y_h(t)}{dt^2} + c_h\frac{dy_h(t)}{dt} + k_h y_h(t) = V_{hL}(t) - V_{hR}(t) \tag{3}$$

where $y_h(t)$ is the vertical displacement of the connecting point of the hanger with the contact wire; m_h, c_h, and k_h denote the effective mass, the effective damping coefficient, and the effective stiffness of the hangers; $V_{hL}(t)$ and $V_{hR}(t)$ denote the forces the hanger receives from the left and right neighbor wires at the connecting point, respectively.

The pantograph is also modeled as a single-degree-of-freedom lumped mass system whose equation of motion is given by

$$m_p\frac{d^2 y_p(t)}{dt^2} + c_p\frac{dy_p(t)}{dt} = F + V_{pL}(t) - V_{pR}(t) \tag{4}$$

where $y_p(t)$ is the vertical displacement of the contact point of the pantograph with the contact wire; m_p, c_p, and F are the effective mass, the effective damping coefficient, and the vertical thrust force of the pantograph; $V_{pL}(t)$ and $V_{pR}(t)$ denote the forces the pantograph receives from the left and right neighbor wires at the contact point, respectively.

2.2. Transfer matrix and its wave component representation

Let us consider a part of the wire of length l. Taking the Laplace transform of equation (1) gives

$$\frac{\partial^2 \hat{y}(x,s)}{\partial x^2} - \frac{s^2}{c^2}\hat{y}(x,s) = g(x,s) \tag{5}$$

$$g(x,s) = -\frac{1}{c^2}\left\{sy(x,0) + \dot{y}(x,0)\right\} \tag{6}$$

where $\hat{(\cdot)}$ denotes the variable in the Laplace domain, $\dot{(\cdot)}$ denotes the temporal derivative, and $c = \sqrt{T/\rho}$. Solving the second-order ordinary differential equation (5), the general solution at arbitrary location is derived as

$$\hat{y}(x,s) = c_1(s)e^{-\frac{s}{c}x} + c_2(s)e^{\frac{s}{c}x} + Y(x,s) \tag{7}$$

where $Y(x,s)$ is the particular solution of equation (5) given by

$$Y(x,s) = h_1(x,s)e^{-\frac{s}{c}x} + h_2(x,s)e^{\frac{s}{c}x} \tag{8}$$

where

$$h_1(x,s) = -\frac{c}{2s}\int_0^x e^{\frac{s}{c}x'}g(x',s)dx' \tag{9}$$

$$h_2(x,s) = \frac{c}{2s}\int_0^x e^{-\frac{s}{c}x'}g(x',s)dx' \tag{10}$$

From equations (7) and (2), the state variables at $x = l$ are derived as a linear function of the state variables at $x = 0$ as

$$\begin{bmatrix} \hat{y}(l,s) \\ \hat{V}(l,s) \end{bmatrix} = \begin{bmatrix} \cosh\left(\frac{s}{c}l\right) & -\frac{c}{Ts}\sinh\left(\frac{s}{c}l\right) \\ -\frac{Ts}{c}\sinh\left(\frac{s}{c}l\right) & \cosh\left(\frac{s}{c}l\right) \end{bmatrix} \begin{bmatrix} \hat{y}(0,s) \\ \hat{V}(0,s) \end{bmatrix} + \begin{bmatrix} Y(l,s) \\ -T\frac{\partial Y(l,s)}{\partial x} \end{bmatrix} \tag{11}$$

where $\hat{y}_p(x,s)$ is the particular solution of equation (5), and

$$\mathbf{T}_w = \begin{bmatrix} \cosh\left(\frac{s}{c}l\right) & -\frac{c}{Ts}\sinh\left(\frac{s}{c}l\right) \\ -\frac{Ts}{c}\sinh\left(\frac{s}{c}l\right) & \cosh\left(\frac{s}{c}l\right) \end{bmatrix} \tag{12}$$

is the transfer matrix. Diagonalization of the transfer matrix leads to the wave component representation as follows:

$$\begin{bmatrix} \hat{w}_f(l,s) \\ \hat{w}_b(l,s) \end{bmatrix} = \mathbf{\Lambda} \begin{bmatrix} \hat{w}_f(0,s) \\ \hat{w}_b(0,s) \end{bmatrix} + \mathbf{\Phi}^{-1} \begin{bmatrix} Y(l,s) \\ -T\frac{\partial Y(l,s)}{\partial x} \end{bmatrix} \tag{13}$$

where $\hat{w}_f(x,s)$ and $\hat{w}_b(x,s)$ are the forward and backward propagating wave components, respectively. The matrices appearing in the right-hand-side are defined as

$$\mathbf{\Lambda} = \begin{bmatrix} e^{-\frac{s}{c}l} & 0 \\ 0 & e^{\frac{s}{c}l} \end{bmatrix} \tag{14}$$

and

$$\mathbf{\Phi} = \begin{bmatrix} 1 & 1 \\ \frac{Ts}{c} & -\frac{Ts}{c} \end{bmatrix} \tag{15}$$

3. Method

3.1. Local coordinate systems and wave components

The contact wire is divided into elements span-by-span. In order to develop an analysis method based on the method of reverberation-ray matrix [11, 12], the following naming rules of joints and elements, and the definition of local coordinate systems are adopted. The connecting points of the hangers and the contact point of the pantograph are considered as joints denoted by letters 0, 1, …, I, J, K, …, $N-1$, N as depicted in figure 1. The element bounded by joints I and J is named element IJ. Because the joint J is the contact point moving in the positive direction, the element IJ and the element JK are time-varying elements with decreasing and increasing length, respectively. Then, two sets of dual local coordinate systems are introduced for each element IJ, with the one located at joint I (labeled by superscript IJ) and the other at joint J (labeled by superscript JI) as illustrated in figure 2.

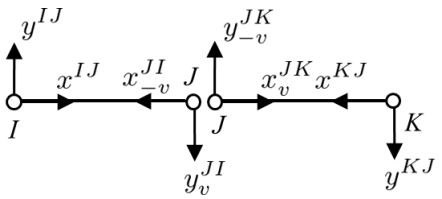


Figure 2. Local coordinate systems.

The wave components traveling on the wire are classified into two groups: departing waves and arriving wave. For each joint J, the wave components departing from J to K and arriving at J from K are designated as d^{JK} and a^{JK}, respectively, as illustrated in figure 3, where all the components related to the elements IJ and JK are schematically denoted.

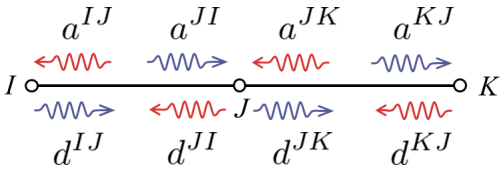


Figure 3. Wave components.

3.2. Phase matrix

For each element IJ, the wave components departing from the joint I will arrive at the joint J, and vice versa. These relationships among the wave components traveling through a certain element are described by a phase matrix.

3.2.1. Time-invariant element Let us consider an element HI with time-invariant length. Rearranging equation (13) and considering the local coordinates, the arriving waves are related to the departing waves and initial conditions as

$$a^{HI}(s) = P^{HI}(s)\, d^{IH}(s) + q^{HI}(s) \tag{16}$$

$$a^{IH}(s) = P^{IH}(s)\, d^{HI}(s) + q^{IH}(s) \tag{17}$$

where

$$P^{HI}(s) = P^{IH}(s) = -e^{-\frac{s}{c}l} \tag{18}$$

and

$$q^{HI}(s) = -\frac{c}{2s}\int_0^l e^{-\frac{s}{c}x'} g^{HI}(x', s)dx' \tag{19}$$

$$q^{IH}(s) = e^{-\frac{s}{c}l}\frac{c}{2s}\int_0^l e^{\frac{s}{c}x'} g^{HI}(x', s)dx' \tag{20}$$

3.2.2. Time-varying element Let us consider the pantograph's contact point J moving with a constant velocity of v and adjacent joints I and K as illustrated in figure 4. Because the elements IJ and JK have time-varying lengths, special treatment is required in handling these elements.

For the stretching element IJ, the wave field is first described in the stationary coordinate IJ as

$$\hat{y}^{IJ}(x^{IJ}, s) = d^{IJ}(s)e^{-\frac{s}{c}x^{IJ}} + a^{IJ}(s)e^{\frac{s}{c}x^{IJ}} \tag{21}$$

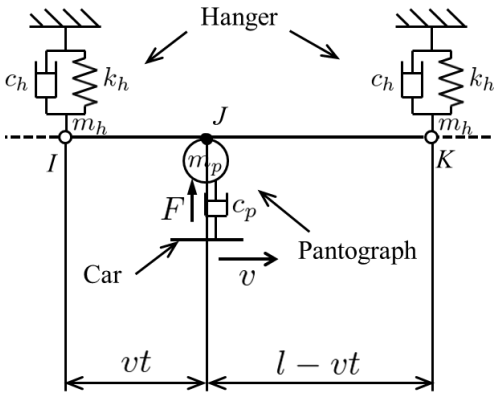


Figure 4. Time-varying elements.

which is obtained from equation (7). Applying a coordinate transformation $x^{IJ} = vt - x^{JI}$ yields an expression of the same field on the moving coordinate JI in the time domain as

$$y^{JI}(x^{JI},t) = -\frac{1}{2\pi i}\int_{\sigma-i\infty}^{\sigma+i\infty}\hat{y}^{IJ}(vt-x^{JI},s')e^{s't}ds' \tag{22}$$

$$= -\frac{1}{2\pi i}\int_{\sigma-i\infty}^{\sigma+i\infty}\left\{d^{IJ}(s')e^{-\frac{s'}{c}(vt-x^{JI})} + a^{IJ}(s')e^{\frac{s'}{c}(vt-x^{JI})}\right\}e^{s't}ds' \tag{23}$$

Taking the Laplace transform again results in

$$\hat{y}^{JI}(x^{JI},s) = -\frac{c}{c+v}\,a^{IJ}\left(\frac{c}{c+v}s\right)e^{-\frac{s}{c+v}x^{JI}} - \frac{c}{c-v}\,d^{IJ}\left(\frac{c}{c-v}s\right)e^{\frac{s}{c-v}x^{JI}} \tag{24}$$

From equation (24), the arriving waves are related to the departing waves as

$$a^{IJ}(s) = P^{IJ}(s)\,d^{JI}\left(\frac{c+v}{c}s\right) \tag{25}$$

$$a^{JI}(s) = P^{JI}(s)\,d^{IJ}\left(\frac{c}{c-v}s\right) \tag{26}$$

where

$$P^{IJ}(s) = -\frac{c+v}{c} \tag{27}$$

$$P^{JI}(s) = -\frac{c}{c-v} \tag{28}$$

Similarly, for the shrinking element JK, the arriving waves are related to the departing waves and initial conditions as

$$a^{JK}(s) = P^{JK}(s)\,d^{KJ}\left(\frac{c}{c+v}s\right) + q^{JK}(s) \tag{29}$$

$$a^{KJ}(s) = P^{KJ}(s)\,d^{JK}\left(\frac{c-v}{c}s\right) + q^{KJ}(s) \tag{30}$$

where

$$P^{JK}(s) = -\frac{c}{c+v}\,e^{-\frac{s}{c+v}l} \tag{31}$$

$$P^{KJ}(s) = -\frac{c-v}{c}\,e^{-\frac{s}{c}l} \tag{32}$$

and

$$q^{JK}(s) = e^{-\frac{s}{c+v}l}\frac{c}{2s}\int_0^l e^{\frac{s}{c+v}x'}g^{KJ}\left(x',\frac{c}{c+v}s\right)dx' \tag{33}$$

$$q^{KJ}(s) = -\frac{c-v}{2s}\int_0^l e^{-\frac{s}{c}x'}g^{KJ}(x',s)dx' \tag{34}$$

Equations (25), (26), (29) and (30) imply that arriving waves at a certain frequency are related to the departing waves at another frequency. This corresponds to the Doppler effect that arises at the contact point of the moving pantograph. Due to this effect, the relationships among wave components in the time-varying elements are not frequency-independent in contrast to the ordinary transfer matrix method and the method of reverberation-ray matrix. Hence, one have to consider augmented vectors $\mathbf{a}^{IJ}$ and $\mathbf{d}^{JI}$ of arriving and departing wave components at discretized Laplace points sampled to calculate the

Bromwich integral for numerical inverse Laplace transform [14, 15]. Thus, equations (25) and (26) can be expressed as

$$\mathbf{a}^{IJ} = \mathbf{P}^{JI}\mathbf{d}^{IJ} \tag{35}$$

and equations (29) and (30) as

$$\mathbf{a}^{JK} = \mathbf{P}^{JK}\mathbf{d}^{KJ} + \mathbf{q}^{JK} \tag{36}$$

Then, all equations can be assembled into the global phase matrix equation as

$$\mathbf{a} = \mathbf{P}\bar{\mathbf{d}} + \mathbf{q} \tag{37}$$

3.3. Scattering matrix

The relationships among the arriving and departing wave at a certain joint are described by the scattering matrix.

For the joint I corresponding to the connecting point of the hanger, the scattering matrix is derived from the transfer matrix representation across the connecting point, which is given by

$$\mathbf{z}^{IH} = \mathbf{T}_h\mathbf{z}^{IJ} + \mathbf{f}_h \tag{38}$$

where

$$\mathbf{T}_h = \begin{bmatrix} -1 & 0 \\ m_h s^2 + c_h s + k_h & 1 \end{bmatrix} \tag{39}$$

$$\mathbf{f}_h = \begin{bmatrix} 0 \\ \hat{f}_h(s) \end{bmatrix} \tag{40}$$

$$\hat{f}_h(s) = (m_h s^2 + c_h s)y_h(0) + m_h\dot{y}_h(0) \tag{41}$$

which is derived via the Laplace transform of the equation of motion (3). Taking the coordinate transformation using the eigenvector matrix $\mathbf{\Phi}$ given by equation (15) leads to an equivalent representation written by the wave components as

$$\mathbf{w}^{IH} = \mathbf{\Phi}^{-1}\mathbf{T}_h\mathbf{\Phi}\mathbf{w}^{IJ} + \mathbf{\Phi}^{-1}\mathbf{f}_h \tag{42}$$

Then, rearranging equation (42) and gathering all the Laplace points in the same way as the previous subsection, one will have the relationship between arriving and departing wave components in the form of

$$\mathbf{d}^I = \mathbf{S}^I\mathbf{a}^I + \mathbf{f}^I \tag{43}$$

where $\mathbf{S}^I$ is called local scattering matrix.

For the joint J corresponding to the contact point of the pantograph, the scattering equation is derived from the transfer matrix representation across the contact point, which is given by

$$\mathbf{z}^{JI} = \mathbf{T}_p\mathbf{z}^{JK} + \mathbf{f}_p \tag{44}$$

where

$$\mathbf{T}_p = \begin{bmatrix} -1 & 0 \\ m_p s^2 + c_p s & 1 \end{bmatrix} \tag{45}$$

$$\mathbf{f}_p = \begin{bmatrix} 0 \\ \hat{f}_p(s) \end{bmatrix} \tag{46}$$

$$\hat{f}_p(s) = (m_p s^2 + c_p s)y_p(0) + m_p\dot{y}_p(0) - \frac{F}{s} \tag{47}$$

which is derived via the Laplace transform of the equation of motion (4). Taking the same way as described above, one will have

$$\mathbf{d}^J = \mathbf{S}^J\mathbf{a}^J + \mathbf{f}^J \tag{48}$$

which is the local scattering equation at the contact point of the pantograph.

Finally, assembling all the local scattering equations, the global scattering matrix equation is derived as

$$\mathbf{d} = \mathbf{S}\mathbf{a} + \mathbf{f} \tag{49}$$

Note that the vectors $\mathbf{d}$ in the above equation and $\bar{\mathbf{d}}$ in equation (37) have the same elements but sequenced in different orders. The relationship between them can be formulated as

$$\bar{\mathbf{d}} = \mathbf{U}\mathbf{d} \tag{50}$$

where $\mathbf{U}$ is the permutation matrix.

3.4. Reverberation-ray matrix

Combining equations (37), (49) and (50) results in

$$\mathbf{d} = (\mathbf{I} - \mathbf{R})^{-1}(\mathbf{S}\mathbf{q} + \mathbf{F}) \tag{51}$$

where $\mathbf{R} = \mathbf{S}\mathbf{P}\mathbf{U}$ is called reverberation-ray matrix [11].

It would be hard to calculate the right-hand-side of equation (51) because the size of the reverberation-ray matrix $\mathbf{R}$ can be huge and the inversion can be ill-posed. Instead, the Neumann series expansion of $(\mathbf{I} - \mathbf{R})^{-1}$ can be applied as suggested by Howard and Pao [11, 12] as follows

$$(\mathbf{I} - \mathbf{R})^{-1} = \mathbf{I} + \mathbf{R} + \mathbf{R}^2 + \ldots + \mathbf{R}^N + \ldots \tag{52}$$

After getting all of the departing waves by calculating equation (51), the arriving waves are derived as

$$\mathbf{a} = \mathbf{P}\mathbf{U}\mathbf{d} + \mathbf{q} \tag{53}$$

It should be noted that multiplying $\mathbf{R}$ by the wave components means to scatter the waves one more time. Thus, truncation of the expansion at $N + 1$-th term implies to take account of wave components which are scattered up to N times.

3.5. Infinite boundary conditions, spatial shift and continuation

In this study, the pantograph is assumed to run along the contact wire with infinite length. Of course only finite number of wave components can be dealt with, the model has to be truncated with finite number of spans. Assuming that the pantograph P is running between the hangers I and J, let us think of a region of interest bounded by hangers $I - M$ and $J + M$. The total span number in the region is $2M + 1$. By taking sufficiently large M, it would be reasonable to assume that the waves incoming from outside of the region of interest are negligibly small. Therefore, at both boundaries of the region, this assumption can be used as the boundary conditions.

As long as the pantograph remains between the hangers I and J, the formulation described in the previous subsections is valid and the responses of the catenary and the pantograph can be calculated. When the pantograph reaches the hanger J and comes into the next span, however, the formulation can no longer be applied because the structural adjacent relation of the pantograph with the hangers changes. Thus, it is necessary to alter the adjacent order from I, P, J, K to I, J, P, K.

In order to avoid the structural alteration, the analysis is interrupted at $t = l/v$ when the pantograph reaches the hanger J. The displacement and velocity of the wire in the region of interest at this moment are derived by inverse Laplace transform. These are shifted backward by one span length, then used as the initial conditions for the next time interval. The initial conditions for the span at the positive end of the region is set to zero. This process is repeated as illustrated in figure 5, going back and force between temporal and Laplace domain.

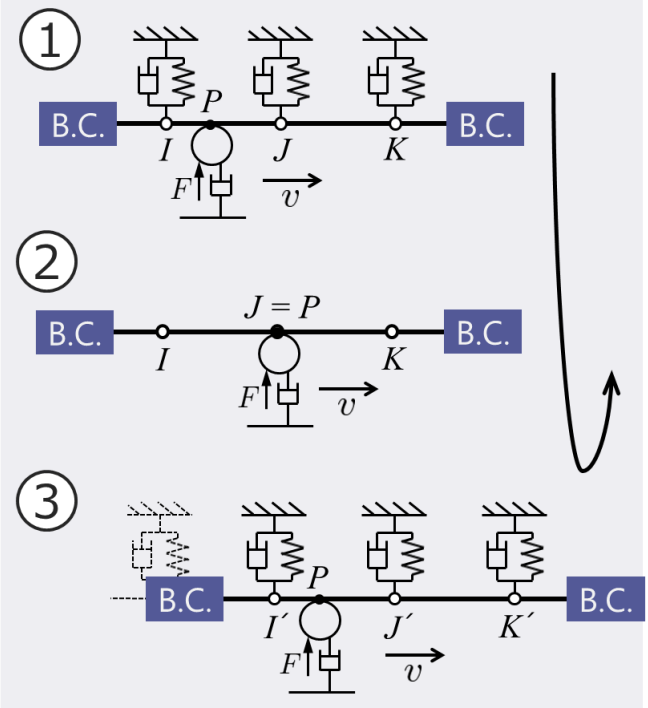


Figure 5. Repetitive spatial shift and continuation.

4. Examples

4.1. Steady-state response of zero-impedance pantograph

In this case, the mass and the damping coefficient of the pantograph are set sufficiently small so that the calculation results are compared with the previous study by Metrikine et al. [4]. The parameter values are listed in Table 1. The analysis was started with zero initial conditions and continued until the response converges to steady-state.

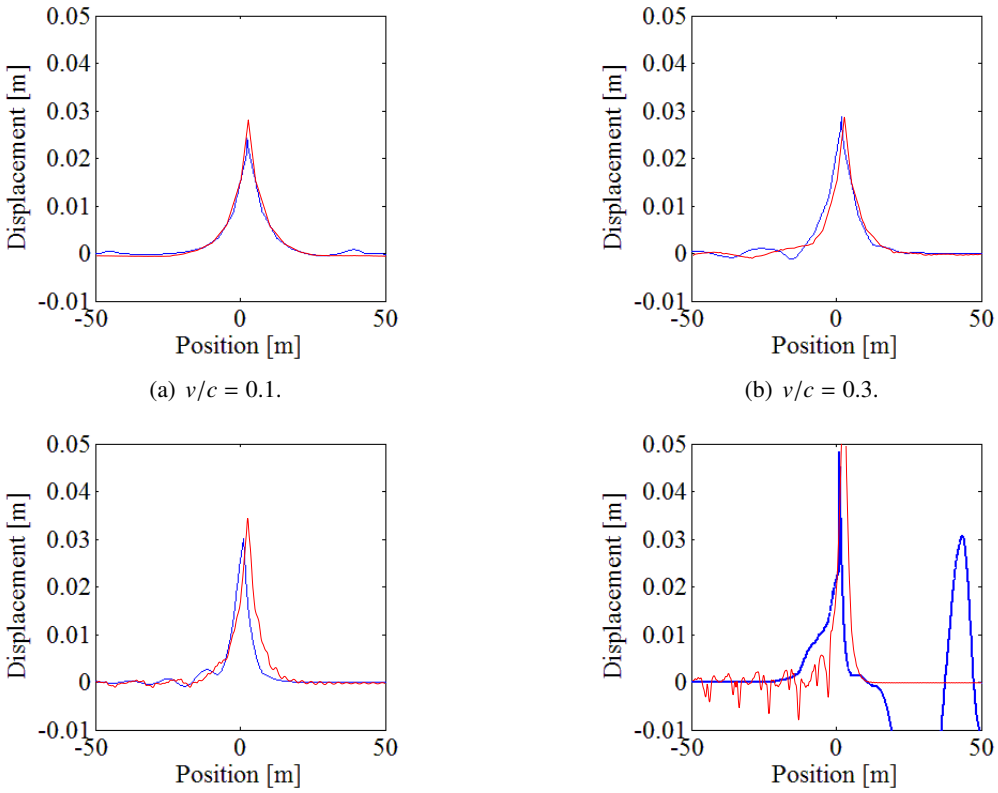
Table 1. Parameter values.

Parameter	Value	Parameter	Value
m_p	10^{-6} kg	m_h	1 kg
c_p	10^{-6} N· s/m	c_h	20 N· s/m
F	100 N	k_h	2000 N/m
c	100 m/s	T	10000 N
l	5 m	M	20 spans

The comparison is shown in figure 6 for various speed ratio v/c. In the figure, the displacement of the contact wire in the steady-state is plotted. The results from the present study are plotted in blue, while the results using the formulation proposed by Metrikine et al. [4] are in red.

Metrikine el al. [4] pointed out two findings:

- When the load velocity was relatively small (up to $v/c = 0.3$), the displacement pattern was almost symmetric with respect to the loading point (pantograph). With increasing velocity the pattern became more and more asymmetric and for $v/c = 0.9$ the displacement before the load became negligibly small.
- Maximum displacement of the wire grew, as the load velocity became higher.



(a) $v/c = 0.1$. (b) $v/c = 0.3$.

(c) $v/c = 0.6$. (d) $v/c = 0.9$.

Figure 6. Displacement of the catenary over 10 span distance from the pantograph. Present study in blue line; results using the formulation proposed by Metrikine et al. [4] in red line.

From figure 6, the present study agrees with these findings apart from the case $v/c = 0.9$, where the displacement before the pantograph is disturbed possibly because of numerical instability of the inverse Laplace transform.

4.2. Transient response of pantograph with impedance

In this case, the parameters of the pantograph are set more realistically as listed in Table 2. Since the pantograph with impedance can interact with the waves propagating on the wire, the multiple scattering and the Doppler effect are fully considered in this analysis. The analysis was started with zero initial conditions and continued until the response converges to steady-state.

Table 2. Parameter values.

Parameter	Value	Parameter	Value
m_p	6 kg	m_h	1 kg
c_p	35 N· s/m	c_h	20 N· s/m
F	73.5 N	k_h	2000 N/m
c	100 m/s	T	10000 N
l	5 m	M	20 spans

The transient displacement responses for $v/c = 0.1$ and $v/c = 0.3$ are shown on spatial-time plane in figure 7. Because the pantograph applies constant upthrust to the catenary, the wire undergoes step input

at $t = 0$. Then, repeating pass-by of the hanger at every 5 m makes the pantograph respond periodically, with wave motion spreading along the wire. Again, the maximum displacement in the steady-state becomes larger as the velocity increases, but the variation of the displacement becomes smaller. These findings have to be further investigated through more comprehensive parameter study in future.

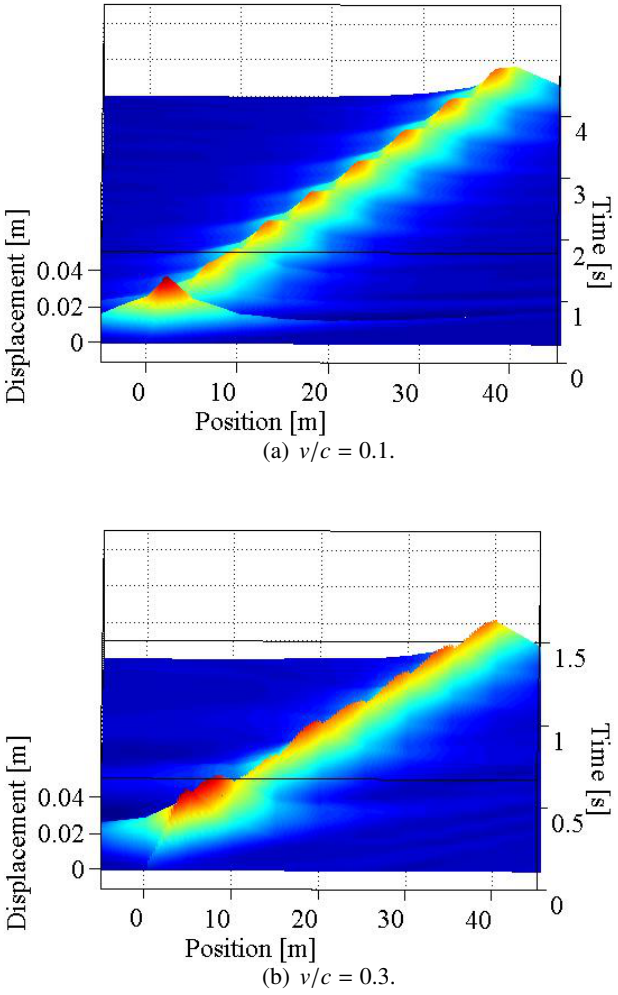


Figure 7. Spatial-time transient response of contact wire.

5. Conclusions

In this paper, a systematic analysis method for the dynamic response of an overhead catenary and a moving pantograph contacting the catenary. The catenary is modeled as a one-dimensional infinite-length string periodically suspended by hangers. The pantograph is modeled as a single-degree-of-freedom structure moving at a constant speed. The whole system is divided into elements, and the relationships among the traveling waves are systematically obtained in the Laplace domain following the method of reverberation-ray matrix. Since the governing equation of the system changes periodically with time, the analysis of the temporal evolution of the system can be realized by repeating a single period analysis inheriting the initial conditions with spatial shifting. Although the qualitative characteristics of the steady-state solutions agreed with those in the previous study, some numerical instability probably

cause by the inverse Laplace transform was observed. The reason for this instability must be fully understood in the future work in order to improve the reliability of the proposed method.

References

[1] Gilbert G and Davies H E H 1966 *Proc. IEE* **113** 3 485–92
[2] Scott P R and Rothman M 1974 *IEEE Trans. Ind. Appl.* **10** 5 573–80
[3] Smith C C and Wormley D N 1975 *J. Dyn. Syst. Meas. Control* **97** 1 21–9
[4] Metrikine A V, Wolfert A F M and Vrouwenvelder A C W M 1999 *HERON* **44** 2 91–107
[5] Metrikine A V and Bosch A L 2006 *J Sound Vib.* **292** 676–93
[6] Kumaniecka A and Smanina J 2008 *J. Theor. Appl. Mech.* **46** 4 869–78
[7] Bitzenbauer J and Dinkel J 2002 *Arch. Appl. Mech.*, **72** 199–211
[8] Shimogo T, Yoshida K and Abe N 1984 *Trans. JSME* C **50** 2292–8
[9] Holzer H 1921 *Die Berechnung der Drehsenwingungen* (Berlin: Springer)
[10] Faulkner M G and Hong D P 1985 *J. Sound Vib.* **99** 1 29-42
[11] Howard S M and Pao Y H 1998 *J. Eng. Mech.* **124** 884–91
[12] Pao Y H, Chen W Q and Su X Y 2007 *Wave Motion* **44** 419–38
[13] Jiang J Q, Chen W Q and Pao Y H 2011 *J. Vib. Control* **18** 6 774–84
[14] Levin D 1975 *J. Comp. Appl. Math.* **1** 4 247–50
[15] Hwang C, Lu M J and Shieh L S 1991 *Comput. Math. Appl.* **22** 1 13–24